Inorganic Chemistry

Article

pubs.acs.org/IC

Lithium Silicide Nanocrystals: Synthesis, Chemical Stability, Thermal Stability, and Carbon Encapsulation

Jacqueline E. Cloud,‡ Yonglong Wang,‡ Xuemin Li, Tara S. Yoder, Yuan Yang, and Yongan Yang*

Department of Chemistry and Geochemistry, Colorado School of Mines, 1012 14th Street, Golden, Colorado 80401, United States

Supporting Information

ABSTRACT: Lithium silicide (Li_xSi) is the lithiated form of silicon, one of the most promising anode materials for the next generation of lithium-ion batteries (LIBs). In contrast to silicon, Li_xSi has not been well studied. Herein we report a facile high-energy ball-milling-based synthesis of four phase-pure Li_xSi (x = 4.4, 3.75, 3.25, and 2.33), using hexane as the lubricant. Surprisingly, the obtained $Li_{3.75}Si$ phase shows significant downward shifts in all X-ray diffraction peak positions, compared with the standard. Our interpretation is that the high-energy ball-mill-synthesized $Li_{3.75}Si$ presents smaller internal pressures and larger lattice constants. The chemical-stability study reveals that only surface reactions occur after $Li_{4.4}Si$ and $Li_{3.75}Si$ are immersed in several battery-assembly-related chemicals. The thermal-stability study shows that $Li_{4.4}Si$ is stable up to 350 °C and $Li_{3.75}Si$ is stable up to 200 °C. This remarkable thermal stability of $Li_{3.75}Si$ is in stark contrast to the long-observed metastability for electrochemically synthesized $Li_{3.75}Si$. The carbon encapsulation of $Li_{4.4}Si$ has also been studied for its potential applications in LIBs.

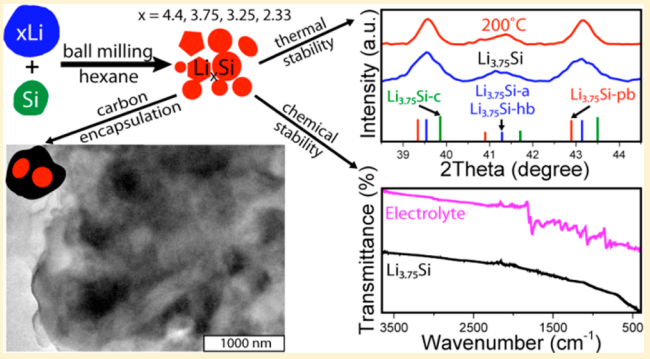

INTRODUCTION

Silicon (Si) has been considered to be one of the most promising anode materials for lithium-ion batteries (LIBs) among all explored candidates because of its ultrahigh theoretical charge capacity of 4200 mAh/g (more than 10 times higher than that of graphite, the current anode in commercial LIBs), earth-abundance, cost-effectiveness, and well-established commercial history.[1−9] However, Si experiences a huge (up to 400%) volume fluctuation as a result of the lithiation process (expansion) to produce lithium silicide alloys (Li_xSi) and the delithiation process (contraction).[1−4,10−13] The volume fluctuation causes two serious issues:[1,14] (1) loss of electrical contact between Si and the current collector due to particle pulverization; (2) repeated deposition/destruction of a shielding layer, the solid electrolyte interphase (SEI), on the electrode surfaces, consuming of the electrolyte solution.[15] Consequently, the charge capacity degrades seriously after only a few cycles.[16,17]

In the past decade, enormous efforts have been invested to gain a deep understanding of the lithiation/delithtion processes.[18−22] It has been found that the initial lithiation converts Si, regardless of crystalline (c-Si) or amorphous (a-Si), to amorphous Li_xSi, until a sudden phase transition from amorphous $Li_{3.75}Si$ to crystalline $Li_{3.75}Si$ occurs, when x reaches 3.75 and the potential goes below 50 mV.[23−25] This electrochemically produced $Li_{3.75}Si$ crystal has been called a metastable phase because of its absence in the Li−Si phase diagram and its instability upon removal from the electrochemical cell.[4,26−30] When the lithiation potential is further lowered, formation of the most Li-rich thermodynamic phase of $Li_{4.4}Si$ has sometimes been reported.[31,32] The resultant volume expansion completely pulverizes the Si particles. During the delithiation process, the volume contraction cannot recover from the damage and may even cause further deterioration. The volume-fluctuation-induced damage has been found to be dependent on the particle size and crystallinity as well as crystalline facets.[4,19,22,24] In contrast to the tremendous studies on Si,[1,7,10,18−22,28,33−37] its lithiated state Li_xSi has barely been investitated.[38−41] The existing publications about Li_xSi mainly focus on electrochemically synthesized *amorphous* Li_xSi (x < 3.75).[38−42] Evidence has been emerging that the electrochemically made Li_xSi behaves differently from the premade Li_xSi by other methods.[28,43] All other thermodynamic phases of Li_xSi (x = 3.25, 2.33, 1.71, and 1.0) have never been observed in electrochemical cells. Therefore, it is of fundamental interest to systematically study Li_xSi, a state that is equally important as Si in an operating LIB.

To date, a number of strategies have been reported to accommodate the volume fluctuation,[6−9,36,44−52] among which the Si@void@C yolk@void@shell nanostructure is very elegant and effective.[6,49] The innovation is to preset a void space surrounding the Si core and inside the carbon (C) shell. With this structure, during the lithiation process, the void space allows for volume expansion inside the shell; during the delithiation process, the void space can be recovered because of

Received: August 6, 2014
Published: September 29, 2014

   dx.doi.org/10.1021/ic501923s | Inorg. Chem. 2014, 53, 11289−11297

volume contraction. In this way, little damage is caused to the C shell and the SEI layer. Consequently, the electrode cyclability is remarkably improved.[6] However, because the void space is preset through a sacrificial matrix, it is very challenging to create the exact volume needed for every particle because of the difficulty of making monodisperse particles. We conjecture that this stringent limitation may be eliminated by making Li_xSi@C core@shell structures. In this approach, the void space is created after the initial electrochemical delithiation with the volume exactly needed for the subsequent lithiation of *x*Li, regardless of the particle size and shape. Thus, highly cyclable Li_xSi electrodes may be achievable. It is therefore of technological importance to explore Li_xSi@C structures.

Because C encapsulation is usually conducted by pyrolyzing polymer precursors at high temperatures (such as 300−600 °C),[53,54] the thermal stability of pure Li_xSi particles needs to be studied first. Such an understanding is also important for mitigating the safety-threatening danger of thermal runaway due to short circuit, possibly causing the temperature to reach 200 °C.[55,56] In addition, it is well-known that an SEI layer can form on the surface of Li_xSi during the process of lithiating Si.[57] For Li metal, an SEI layer can be formed immediately just in contact with electrolyte solutions.[58] The SEI layer plays a crucial role in cyclability because, on the one hand, it slows down the Li-ion diffusion and, on the other hand, it stabilizes the electrode.[58] Thus, it is important to systematically study the chemical stability of Li_xSi with battery-assembly-related chemicals.

This article reports the synthesis of four phase-pure Li_xSi (x = 4.4, 3.75, 3.25, and 2.33) nanocrystals, which are characterized by X-ray diffraction (XRD), solid-state ^{7}Li NMR, transmission electron microscopy (TEM), and energy-dispersive X-ray (EDX) spectroscopy. The chemical and thermal stabilities of $Li_{4.4}Si$ and $Li_{3.75}Si$ have been systematically studied. In addition, the C encapsulation of $Li_{4.4}Si$ has also been conducted.

RESULTS AND DISCUSSION

Synthesis. *Methodology Exploration.* To date, three methods have been reported to synthesize Li_xSi: melt quenching,[26,59] electrochemical lithiation,[34,43] and mechanical ball milling.[28,60−63] Melt quenching is the method used to establish the Li−Si phase diagram, which identifies five thermodynamically stable phases of Li_xSi (x = 4.4, 3.25, 2.33, 1.71, and 1.0).[26,59] The equipment and operation in this method are fairly sophisticated, making it undesirable for scalable production. Electrochemical lithiation inevitably introduces SEI layers on the surface and can only produce $Li_{4.4}Si$ and $Li_{3.75}Si$.[34,43] Mechanical ball milling, classified as planetary ball milling and high-energy ball milling, can directly synthesize $Li_{3.75}Si$; if further combined with postannealing, it can also produce thermodynamically stable phases.[28,60−63] However, the obtained products are usually not phase-pure.[28,60−63] In addition, dodecane, the lubricant typically used to assist in uniform milling, is viscous and has a high boiling point of 216 °C, making postpurification difficult.[61] Thus, overall, ball milling is an attractive method for laboratory research; however, it is critical to improving the phase purity and search for an alternative lubricant.

Considering the high activity of Li and Li_xSi, which react with most polar solvents, our limited choices of alternative lubricants were two hydrocarbons, toluene and hexane, with dodecane as a comparison. The molar ratio of Li/Si in the loading precursors in this subsection was always 4.4/1, unless otherwise stated. The XRD characterization in Figure 1 showed that none

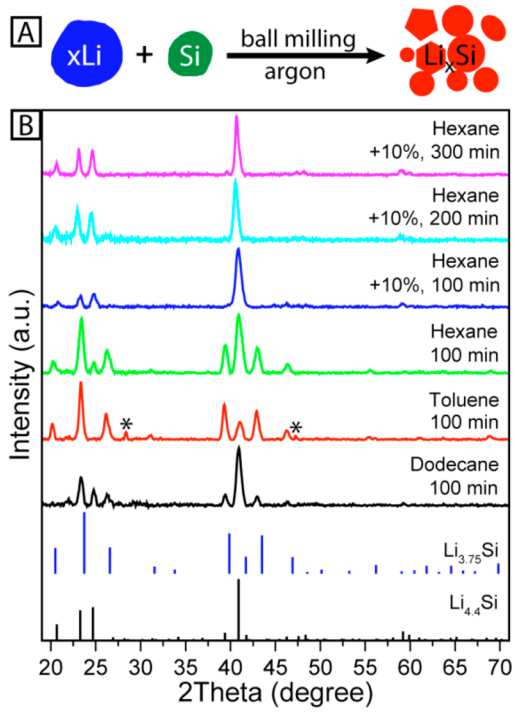

Figure 1. Demonstration of the synthetic method and the condition optimization for synthesizing Li_xSi. (A) Scheme illustrating the high-energy ball-milling process using Li grains and Si powders as precursors. (B) XRD data of the high-energy ball-milled products using different lubricants at the molar ratio of Li/Si = 4.4/1: (black) dodecane, 100 min; (red) toluene, 100 min; (green) hexane, 100 min; (blue) hexane, 10% of extra Li, 100 min; (cyan) hexane, 10% of extra Li, 200 min; and (pink) hexane, 10% of extra Li, 300 min. The asterisked peaks are from unreacted Si. The stick patterns are for standards of $Li_{4.4}Si$ (black; JCPDS 04-007-0820) and $Li_{3.75}Si$ (blue; JCPDS 04-015-2208).

of the directly ball-milled products out of these three lubricants were phase-pure $Li_{4.4}Si$. In the case of dodecane (black), the strongest peak at 40.80° and the two medium peaks at 23.22° and 24.65° indicated the major product as $Li_{4.4}Si$. The small peaks at 26.42° and 43.08° implied the coexistence of a tiny amount of $Li_{3.75}Si$. In the case of toluene (red), the relative positions and intensities of all seven major diffraction peaks (20.43°, 23.52°, 26.42°, 39.60°, 41.34°, 43.08°, and 55.66°) coincided with the features of $Li_{3.75}Si$, except the asterisked ones that were assigned to unreacted Si. The slight and systematic shifts in the absolute peak positions will be discussed later. The hexane system (green) presented products similar to those of the dodecane system, that is, mainly $Li_{4.4}Si$ and a small amount of $Li_{3.75}Si$. From these results, our conjecture was that the reaction might need a longer milling time, postannealing, or excess Li. After the milling time was prolonged to 800 min for the dodecane system, pure $Li_{4.4}Si$ was indeed obtained (see the Supporting Information, SI-Figure 1). However, after annealing at 450 °C for 720 min, as reported in the literature for synthesizing $Li_{4.4}Si$ from planetary ball-milled precursors,[28] we obtained $Li_{3.25}Si$; when using an extra 10% of Li, the products were still a mixture of $Li_{4.4}Si$ and $Li_{3.75}Si$ (see the Supporting Information, SI-Figure 1). In contrast, in the case of hexane, the addition of an extra 10% of Li produced pure $Li_{4.4}Si$, regardless

dx.doi.org/10.1021/ic501923s | Inorg. Chem. 2014, 53, 11289−11297

of the milling time from 100 to 300 min (blue, cyan, and pink in Figure 1). While the reason for the difference between our findings and the literature report was unknown and beyond the scope of this work, a possible factor was the different ball-milling apparatuses, that is, high-energy ball mill in this work and planetary ball mill in the literature.[28]

In addition to using Li and Si, another protocol attempted was to use lithium hydride (LiH) powders instead of Li grains, referring to a literature report for synthesizing $Li_{1.71}Si$.[62] The advantage of using LiH over Li lies in not requiring a lubricant during the milling process. However, as shown in the Supporting Information, SI-Figure 2, there was no reaction between LiH and Si after 100 or 500 min of ball milling. Further annealing of the 500 min sample at 600 °C for 1 h produced a mixture of $Li_{3.25}Si$ and $Li_{2.33}Si$. Similar results have also been reported in the literature for synthesizing Li_xGe from LiH and Ge.[64] Therefore, we chose the hexane-based ball-milling method to synthesize other Li_xSi phases.

Recently, there has been some debate about the exact chemical composition of the most Li-rich phase. In 2013, Zeilinger et al. employed the melt-quenching method and prepared single crystals of the most Li-rich phase after isothermal centrifugation.[65,66] They debated that the phase was $Li_{4.25}Si$ instead of the long-believed $Li_{4.4}Si$, while the XRD patterns for these two compounds are identical.[65,66] To simplify the discussion and literature citations in this article, we use the term $Li_{4.4}Si$.

Characterization. Figure 2A shows the XRD data of the obtained phase-pure Li_xSi (x = 4.4, 3.75, 3.25, and 2.33). The

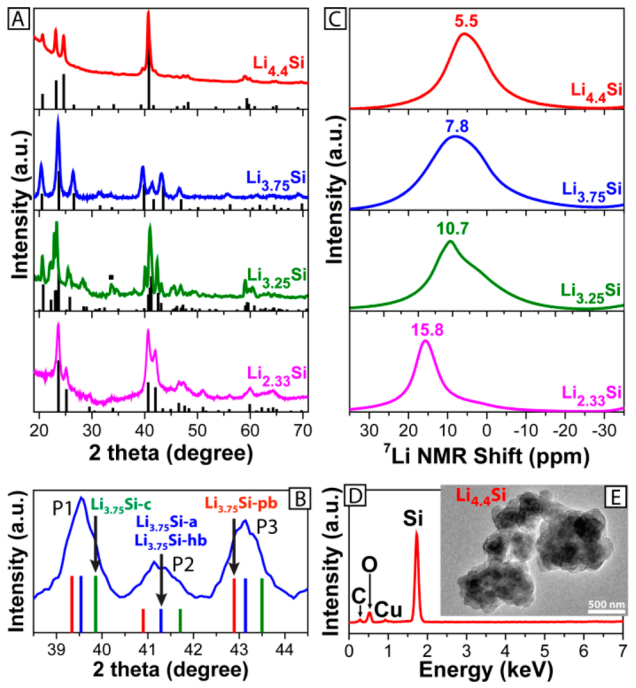

Figure 2. Characterization of various Li_xSi compounds synthesized using the high-energy ball-milling technique. (A) XRD patterns together with stick patterns for standards of $Li_{4.4}Si$ (black; JCPDS 04-007-0820), $Li_{3.75}Si$ (blue; JCPDS 04-015-2208), $Li_{3.25}Si$ (green; JCPDS 00-029-0830), and $Li_{2.33}Si$ (pink; JCPDS 01-089-000). (B) Zoom-in on the range of [38.5°, 44.5°] for $Li_{3.75}Si$ with three sets of references: $Li_{3.75}Si$-c (green; JCPDS 04-015-2208), $Li_{3.75}Si$-hb and $Li_{3.75}Si$-a (blue), and $Li_{3.75}Si$-pb (red).[28−30,68,69] (C) Solid-state ^7Li NMR spectra. (D) EDX spectrum of $Li_{4.4}Si$. (E) TEM image of $Li_{4.4}Si$.

crystal sizes calculated for $Li_{4.4}Si$, $Li_{3.75}Si$, $Li_{3.25}Si$, and $Li_{2.33}Si$, using the Scherrer equation, are 13, 15, 14, and 14 nm, respectively.[67] Except for $Li_{3.75}Si$, all other products were obtained by using 10% of extra Li beyond the stoichiometric ratios in the loading precursors. The metastable phase $Li_{3.75}Si$ was directly synthesized through ball milling for 100 min. Surprisingly, as aforementioned briefly, the peak positions (but not the relative intensities) for all diffraction peaks in our experimental data of $Li_{3.75}Si$ (blue) were shifted downward significantly, compared with the standard (JCPDS 04-015-2208) in the XRD database.[30] A zoom-in on the range of [38.5°, 44.5°] was graphed in Figure 2B, together with the stick patterns of crystalline $Li_{3.75}Si$ synthesized through four different methods: electrochemical lithiation of c-Si (denoted as $Li_{3.75}Si$-c),[30] electrochemical lithiation of a-Si ($Li_{3.75}Si$-a),[29,68] planetary ball milling of Li and c-Si ($Li_{3.75}Si$-pb),[28] and high-energy ball milling of Li and c-Si ($Li_{3.75}Si$-hb).[69] Interestingly, the downward shift of all XRD peaks in $Li_{3.75}Si$-pb are even larger.[28] However, there has not been any interpretation about this discrepancy in the literature. In 2013, Zeng et al. reported a continuous upward shift of all XRD peaks (P1−P3) of $Li_{3.75}Si$-c with increasing externally applied pressure (see the Supporting Information, SI-Figure 3).[43] In addition, they also calculated the fractional change of the unit cell volume [V_p/V_0, where V_p is the volume under pressure (P) and V_0 is the volume under no pressure].[43] Referring to this study,[43] we conclude that $Li_{3.75}Si$ made by different methods possesses different lattice constants (internal pressures), increasing (decreasing) in the order of $Li_{3.75}Si$-c, $Li_{3.75}Si$-a ≈ $Li_{3.75}Si$-hb, and $Li_{3.75}Si$-pb. $Li_{3.75}Si$-hb in Figure 2A seems to present less internal pressure by ∼0.7 GPa than $Li_{3.75}Si$-c. The underlying reason to explain our conclusion was that the Si particles in both milling techniques are mobile in a large space, but the high-energy ball-mill-based lithiation generates stronger collision forces, while the Si particles in the electrochemical lithiation processes are immobilized in a confined space. The correlation of the lattice constants of $Li_{3.75}Si$ with the synthetic methods may clarify the puzzling observation of different ^7Li chemical shifts in NMR spectra between $Li_{3.75}Si$-pb (∼6 ppm) and $Li_{3.75}Si$-c (∼10 ppm)[28] because ^7Li NMR is sensitive to the local environments of Li ions.

For $Li_{3.25}Si$, however, the directly milled product was a mixture of $Li_{3.75}Si$ and Si (see the Supporting Information, SI-Figure 4, blue). When 10% of extra Li was added, the product was $Li_{3.75}Si$ (see the Supporting Information, SI-Figure 4, green). After the milled product was annealed at 600 °C for 1 h under argon, the previously obtained sample became pure $Li_{3.25}Si$ (Figure 2A, green). The peak at 33.8° (■) was ascribed to Si due to phase segregation of a trace amount of amorphous Si during the thermal-annealing process. If this peak were from $Li_{2.33}Si$, we would expect to observe serious peak distortions and/or shifts in the ranges of 23−25° and 40−42° because the peaks of $Li_{2.33}Si$ in these ranges are much stronger than the peak at ∼33.8°. However, we did not observe such a phenomenon; instead, all other peaks were consistent with the $Li_{3.25}Si$ standard. The $Li_{2.33}Si$ phase could be directly produced via ball milling but only if 10% of extra Li was added (Figure 2A, pink); otherwise, there was some unreacted Si (see the Supporting Information, SI-Figure 4, red). Similarly, a mixture of $Li_{2.33}Si$ and Si was also observed for the attempt of synthesizing $Li_{1.71}Si$ (see the Supporting Information, SI-Figure 4, black). We did not pursue this compound further because

dx.doi.org/10.1021/ic501923s | Inorg. Chem. 2014, 53, 11289−11297

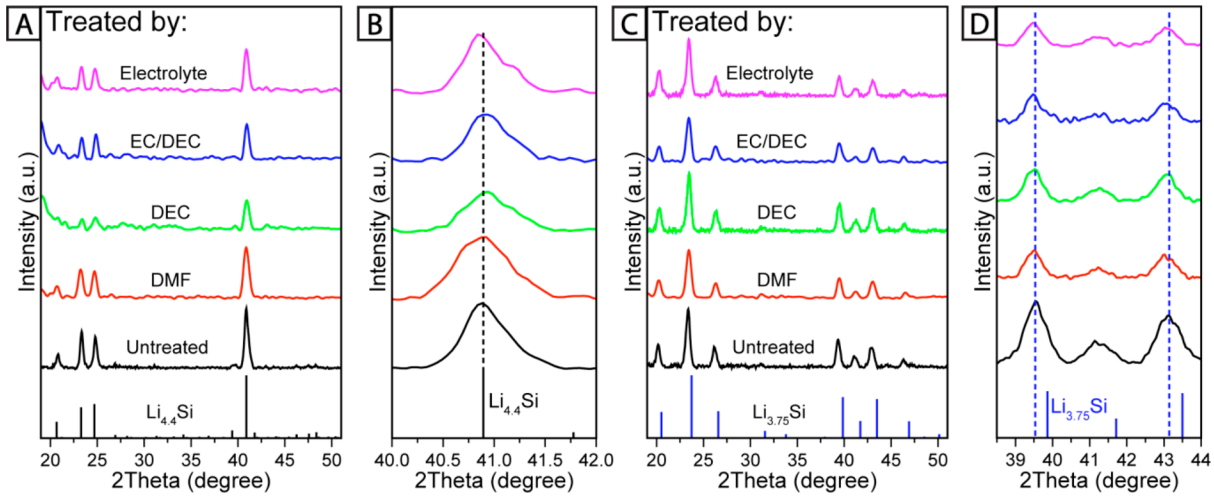

Figure 3. XRD characterization of untreated and DMF-, DEC-, EC/DEC-, and electrolyte-treated $Li_{4.4}Si$ (A and B) and $Li_{3.75}Si$ (C and D), where parts B and D magnify the ranges of 40−42° for $Li_{4.4}Si$ and 38.5−44° for $Li_{3.75}Si$, respectively. The stick patterns are for standards of $Li_{4.4}Si$ (black; JCPDS 040-007-0820) and $Li_{3.75}Si$ (blue; JCPDS 04-015-2208).

the literature showed it could only be produced by annealing the high-energy ball-milled mixture of LiH and Si.[62]

All obtained phase-pure Li_xSi compounds were also characterized by solid-state ^7Li NMR, which showed the expected spectra as reported in the literature (Figure 2C).[28,61] The peak at ∼6 ppm was assigned to Li^+ ions that are bonded to isolated Si ions, and the peak at ∼16 ppm was assigned to Li^+ ions that are bonded to small Si clusters that contain Si−Si bonds.[28,61] The peaks in between indicated the coexistence of both structures.[28]

The EDX spectrum in Figure 2D confirmed the existence of Si (Li is unfortunately not detectable by EDX), in addition to C and copper (Cu) from the TEM grid and oxygen (O) from a slight oxidation of $Li_{4.4}Si$ and surface oxide on the Cu grid. The fact that there were no signals at 0.7 and 6.4 keV confirmed the effective removal of iron (Fe) using a magnet. The TEM image in Figure 2E showed the aggregated morphology of the $Li_{4.4}Si$ nanocrystals.

Chemical Stability of $Li_{4.4}Si$ and $Li_{3.75}Si$. $Li_{4.4}Si$ and $Li_{3.75}Si$ are the only two crystalline phases that are observed in electrochemical cells.[23−25,31,32] It is not surprising that $Li_{4.4}Si$ and $Li_{3.75}Si$ are very reactive because of their alloyed nature. Two videos available in the Supporting Information show that $Li_{4.4}Si$ can catch fire instantly when exposed to air and water. Moreover, we also observed that these two chemicals reacted violently (releasing smoke and sparks) with a number of chemicals including acids, alcohols, *N*-methyl-2-pyrrolidone, dimethoxyethane, nitromethane, and benzonitrile. It has also been widely observed that an insulating SEI layer is formed during the lithiation process of Si, that is, in the process of forming $Li_{4.4}Si$ and $Li_{3.75}Si$. The SEI formation has been assigned to the (electro)chemical reduction of the electrolyte solution on the Li_xSi surfaces.[14,15,70−72] Thus, it is important to understand the chemical stability of $Li_{4.4}Si$ and $Li_{3.75}Si$, particularly in electrolyte environments. In addition, the standard slurry technique for electrode fabrication and carbon encapsulation uses a polar solvent, *N*,*N*-dimethylformamide (DMF).[35] The chemicals tested in this work were the LP40 electrolyte [1 M of $LiPF_6$ in 1/1 (w/w) of ethylenecarbonate/diethylcarbonate (EC/DEC)], DEC, EC/DEC, and DMF. Both $Li_{4.4}Si$ and $Li_{3.75}Si$ were soaked in these chemicals overnight and then characterized by XRD and Fourier transform infrared (FTIR) spectroscopy.

XRD. The first analysis was to study whether the chemical treatment had damaged the crystal structure. The XRD data in Figure 3A,B showed that there was no appreciable change in the crystal structure of $Li_{4.4}Si$ treated by all chemicals, based on the analysis of both the peak positions and the relative intensities in the wide-range (19−51°) and narrow-range (40−42°) diffraction profiles. For $Li_{3.75}Si$ (Figure 3C,D), the crystal structure did not change either as determined by analysis of both the peak positions and the relative intensities in the wide-range (19−51°) and narrow-range (38.5−44°) diffraction profiles. The reason for the peak shift herein was the same as that in the section discussing Figure 2B; that is, $Li_{3.75}Si$ made by different methods possesses different lattice constants (internal pressures), causing all XRD peaks in our experimental data to shift downward compared to the standard (blue sticks, JCPDS 04-015-2208). Since XRD is a technique for analyzing the bulk of the sample because of its large X-ray penetration depth, it is unable to provide surface information. Therefore, a surface technique, FTIR, was further employed.

FTIR. The FTIR spectra for untreated $Li_{4.4}Si$ and $Li_{3.75}Si$ did not show any obvious features, except for a curved background, which is a typical feature for electrical conductors.[73] Referring to the standard spectra of the four chemicals used (DMF, EC, DEC, and pure $LiPF_6$; see the Supporting Information, SI-Figure 5), we concluded that there was no appreciable change to the treated $Li_{4.4}Si$ (Figure 4A), except for DMF. In contrast, for $Li_{3.75}Si$ (Figure 4B), both EC/DEC- and electrolyte-treated $Li_{3.75}Si$ presented peak features from EC (but not DEC because the DEC-treated $Li_{3.75}Si$ did not show a significant change), such as the C═O double bond at about 1780 cm^{-1} and the C−O bond at 1050 cm^{-1}. These results indicate that EC can generate an SEI layer on the surface of $Li_{3.75}Si$ and not on $Li_{4.4}Si$, consistent with the inferior thermodynamic stability of $Li_{3.75}Si$ compared to $Li_{4.4}Si$. In contrast, in the case of DMF, there were surface reactions for both $Li_{3.75}Si$ and $Li_{4.4}Si$ probably because of coordination reactions between the electron-deficient Li ions in Li_xSi and the electron-rich O (and/or N) atoms in DMF.

Thermal Stability of $Li_{4.4}Si$ and $Li_{3.75}Si$. As previously mentioned, $Li_{4.4}Si$ and $Li_{3.75}Si$ are the two most Li-rich phases

dx.doi.org/10.1021/ic501923s | *Inorg. Chem.* 2014, 53, 11289−11297

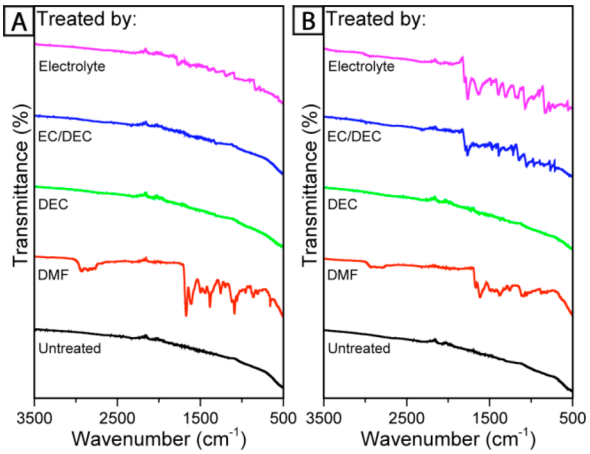

Figure 4. FTIR characterization of untreated and DMF-, DEC-, EC/DEC-, and electrolyte-treated $Li_{4.4}Si$ (A) and $Li_{3.75}Si$ (B).

observed at the end of the electrochemical lithiation of Si, presenting high charge capacities of 4200 and 3579 mAh/g, respectively.[4] Their thermal stability is crucial for the operation of practical LIBs and C encapsulation via pyrolysis.[6,55,56] In this study, XRD was employed to systematically investigate these two samples after they were annealed at several different temperatures and time durations.

$Li_{4.4}Si$. The heating temperatures were 200−600 °C; the heating durations were 1, 6, and 12 h. In the series of 1 h duration (Figure 5A and Supporting Information, SI-Figure 6A), no appreciable change could be observed for 200−350 °C. At 400 °C, a shoulder peak at 41.34° evolved out of the most intense peak (40.80°) of $Li_{4.4}Si$. This emerging peak could be indexed to a combination of two peaks at 41.30° and 41.48° in $Li_{3.25}Si$. In addition, another small peak emerged at 33.80° (■) that was indexed to Si. This peak also showed up at higher temperatures. The phase transition with annealing was assigned to the alloyed nature of Li_xSi and the crystal size effect.[74] The Li in Li_xSi exists more like atoms rather than ions.[28] At the nanometer scale, such Li atoms (whose bulk counterpart melts at 180 °C) can be evaporated, even if the heating temperatures are lower than the melting point of bulk $Li_{4.4}Si$ at 620 °C.[26] The decreased melting points in nanomaterials versus their bulk counterparts have been widely observed.[74] Concomitantly, the loss of Li resulted in the less Li-rich phase of $Li_{3.25}Si$, as observed. At 500−600 °C, the most intense peak originally centered at 40.80° shifted to 40.99°, attributed to the coexistence of the newly formed $Li_{3.25}Si$ with an intense peak at 41.09°. The change in the peak positions in the range of 20−25° were difficult to differentiate because of an additional factor of background correction from the mineral oil used for surface protection.

Very similar trends were observed for the heating durations of 6 and 12 h shown in Figure 5B,C, respectively; although the shoulder peak at ∼41.34° began to appear at 300 °C and became clear at 350 °C in the case of the 12 h duration. At 500 °C, in Figure 5C, a substantial amount of $Li_{4.4}Si$ was converted to $Li_{3.25}Si$. The most intense peak shifted to 40.95°, a broad peak appeared at 41.34°, matching the peaks at 41.30° and 41.48° for $Li_{3.25}Si$, and a peak at 42.59° could be assigned to the peak at 42.61° for $Li_{3.25}Si$. Moreover, the most intense peak for $Li_{3.25}Si$ located at 23.62° could be clearly identified at 23.59°. This peak overlapped with the one from $Li_{4.4}Si$ at 23.27° and became very clear only in the case of 500 °C for 12 h. Note that this peak is not as intense as it should be because of background correction. Attempts at annealing $Li_{4.4}Si$ at 600 °C for 6 and 12 h failed; the product after 6 h was absorbed on the container wall and could not be collected, and after 12 h, the container could not be opened. This thermal stability study shows that $Li_{4.4}Si$ is stable below 350 °C and changes to $Li_{3.25}Si$ at a substantial amount upon reaching 500 °C. This implies that the

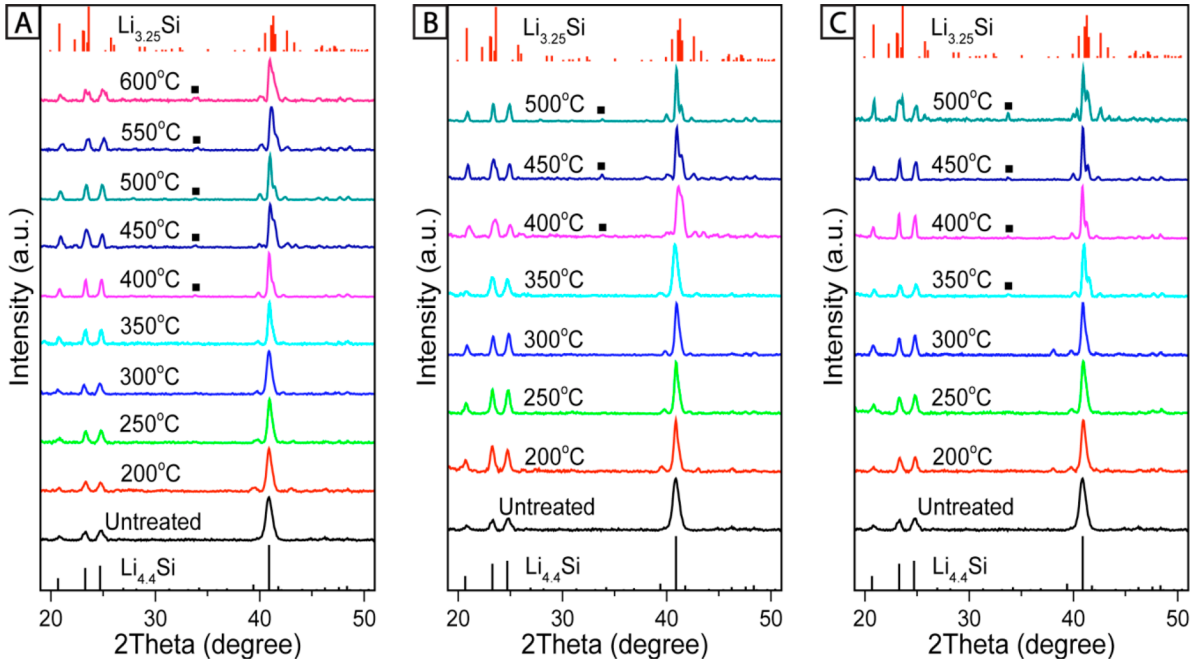

Figure 5. XRD characterization of thermally annealed $Li_{4.4}Si$ at various temperatures for three durations of 1 h (A) 6 h (B), and 12 h (C). The symbol (■) is indexed to Si (JCPDS 04-002-2835). The standard stick patterns are for $Li_{4.4}Si$ (black; JCPDS 04-007-0820) and $Li_{3.25}Si$ (red; JCPDS 01-079-5587).

dx.doi.org/10.1021/ic501923s | *Inorg. Chem.* 2014, 53, 11289−11297

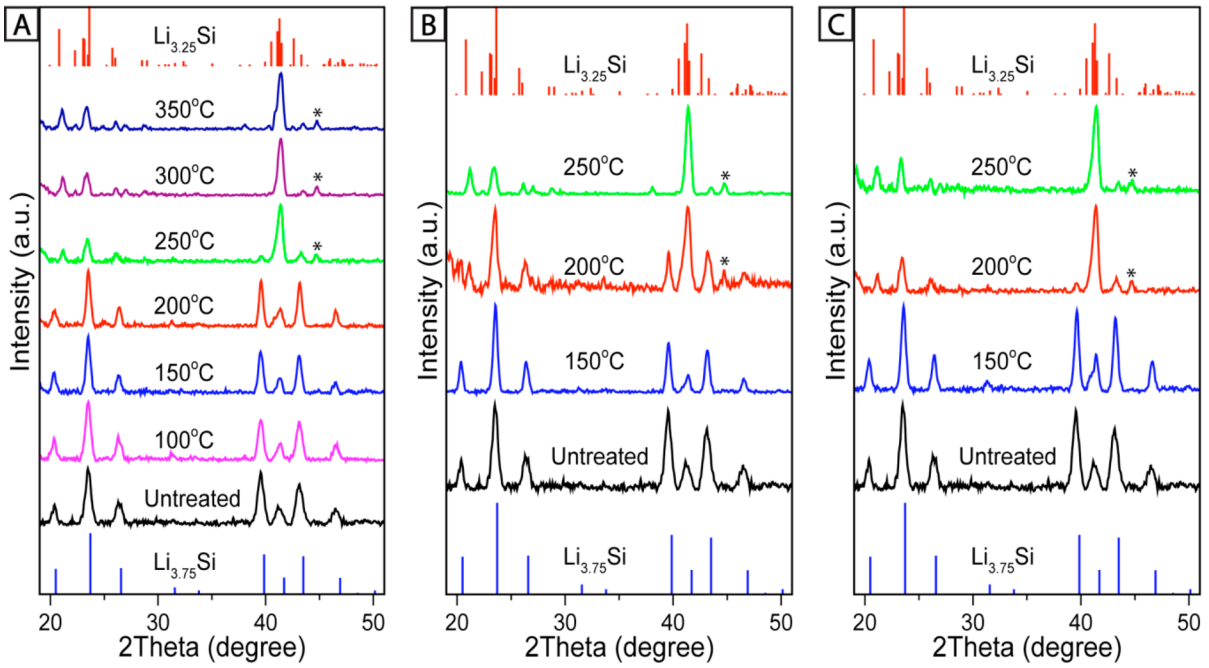

Figure 6. XRD characterization of thermally annealed $Li_{3.75}Si$ at various temperatures for three durations of 1 h (A), 6 h (B), and 12 h (C). The asterisks indicate peaks indexed to Fe (JCPDS 00-003-1050). The standard stick patterns are for $Li_{3.75}Si$ (blue; JCPDS 04-007-0820) and $Li_{3.25}Si$ (red; JCPDS 04-015-2208).

typical pyrolysis process for preparing C encapsulation at temperatures above 600 °C will destroy $Li_{4.4}Si$; a lower (≤350 °C) temperature technique may be more promising. Nevertheless, this study indicates that $Li_{4.4}Si$ will be stable in the case of thermal runaway.

$Li_{3.75}Si$. It has long been believed that $Li_{3.75}Si$ is a metastable phase because it does not exist in the Li−Si phase diagram and loses its crystallinity upon removal from the electrochemical cell.[4,26−30] Surprisingly, as shown in Figure 6A and the Supporting Information, SI-Figure 6B, the high-energy ball-milled $Li_{3.75}Si$ in this work was actually stable even after being heated at ≤200 °C for 1 h. At 250 and 300 °C, the majority of $Li_{3.75}Si$ was transformed to $Li_{3.25}Si$; at 350 °C, the transformation was complete. The evidence for this phase transition was a series of shifts in the peak positions and a change in the relative intensities, that is, from 39.54° to 39.59° (weakened), from 41.14° to 41.34° (intensified), and from 43.14° to 43.29° (weakened). The center peak at 41.34° was most likely a combination of three closely positioned peaks from $Li_{3.25}Si$, located at 41.09°, 41.29°, and 41.48°, respectively. At 250 °C, there was a small amount of $Li_{3.75}Si$ remaining featured by two small peaks at 39.59° and 43.34°. At 350 °C, these peaks shifted to 39.90° and 43.54°, resulting from $Li_{3.25}Si$. The change in the peak positions and intensities was also observed in the range of 20−30°. The asterisked peak was assigned to an Fe contaminant, which came from the milling jar and grew into small particles at elevated temperatures. The Fe impurity should be either in crystal lattices or in grain boundaries. If the former case were true, Fe incorporation would have increased the lattice constants and caused blue shifts of the XRD peaks in all of the Li_xSi samples; however, we did not observe such phenomena (Figure 2A). The experimental data indicated that the latter case was true and the Fe impurity did not play a role in stabilizing $Li_{3.75}Si$-hb. When the annealing duration was extended to 6 h (Figure 6B), the phase transition started at 200 °C and finished at 250 °C. In the case of 12 h (Figure 6C), the phase transition occurred almost completely by 200 °C, except for two small peaks at 39.54° and 43.14°. This study indicated that the high-energy ball-mill-synthesized $Li_{3.75}Si$ is remarkably stable, which we believe is due to the more relaxed lattices compared with the electrochemically synthesized $Li_{3.75}Si$-c. Although some researchers have also reported that $Li_{3.75}Si$-c could be detected by ex situ techniques,[43,68,75] this work has for the first time systematically studied the thermal stability of $Li_{3.75}Si$.

C Encapsulation. The thermal-stability study has revealed that (1) it is impossible to produce a $Li_{3.75}Si$@C composite because $Li_{3.75}Si$ is not stable in the temperature range of 300−600 °C for C encapsulation, (2) it is unfeasible to synthesize a $Li_{4.4}Si$@C composite at 600 °C, and (3) it may be feasible to make a $Li_{4.4}Si$@C composite at 300−350 °C. The feasibility was first tested by pyrolyzing the mixture of $Li_{4.4}Si$ powder and polyacrylonitrile (PAN) powder. After being heated at 600 °C for 1 h (Supporting Information, SI-Figure 7), $Li_{4.4}Si$ was converted to $Li_{3.25}Si$, $Li_{2.33}Si$, Li_2C_2, and Li_2O. After being heated at 300 °C for 1 h (Supporting Information, SI-Figure 7), $Li_{4.4}Si$ was converted to a mixture of $Li_{3.25}Si$ and $Li_{2.33}Si$, confirming the compatibility between $Li_{4.4}Si$ and PAN. Subsequently, a slurry made by dispersing $Li_{4.4}Si$ powder in a DMF solution of PAN was heated at 300 °C for 1 h to partially carbonize PAN to produce a mechanically resilient C (denoted as RC) matrix.[35] Surprisingly, XRD data of the obtained product (Figure 7A) showed that $Li_{4.4}Si$ was converted to $Li_{2.33}Si$. The Raman spectrum of the $Li_{2.33}Si$@RC composite in Figure 7B shows the expected characteristic D band (1378 cm^{-1}) and G band (1584 cm^{-1}), which are comparable to the literature results[35] and indicated the high quality of the RC matrix. The TEM image in Figure 7C illustrated the desired c encapsulation (the light area) of the produced $Li_{2.33}Si$ particles (the dark spots). We conjecture that the "lost" Li was absorbed by the RC matrix and not evaporated out of the system because $Li_{4.4}Si$ has been proven stable at 300 °C and the melting point

dx.doi.org/10.1021/ic501923s | Inorg. Chem. 2014, 53, 11289−11297

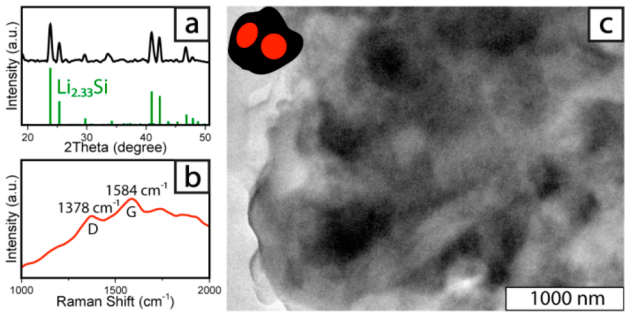

Figure 7. Characterization of the obtained product after pyrolysis of the slurry made from $Li_{4.4}Si$ powder, PAN, and DMF: (A) XRD pattern; (B) Raman spectrum; (C) TEM image, in which the inset conceptually illustrates the C encapsulation of the produced $Li_{2.33}Si$ particles.

of its bulk counterpart is 620 °C.[26,74] If so, the lithiated RC matrix will not be detrimental because the RC matrix will need to be lithiated anyway in an operating battery.[35] Therefore, while this phase degradation is unfortunate, we believe that the resultant $Li_{2.33}Si$@RC composite may still present a high performance, considering three facts: (1) It has been widely accepted that it is practically desirable to cycle at $x < 3.75$ because of the cyclability-killing involvement of $Li_{3.75}Si$ during the lithiation/delithiation cycles.[76−78] (2) The RC matrix has been demonstrated to significantly enhance the cyclability of Si particles[35] because of its capability of accommodating volume fluctuation. Thus, in the case of $Li_{2.33}Si$@RC, the RC matrix is expected to compensate for the deficient void space provided by Li, allowing for a smaller x in Li_xSi at the beginning while cycling at a larger x in reality. (3) The electrode performance would still be remarkable, even if only 80% of the theoretical charge capacity of $Li_{2.33}Si$ (2200 mAh/g) could be retained. Our future tasks are to fabricate electrodes and evaluate their performance.

CONCLUSIONS

This article has reported a systematic study on the synthesis and characterization of a series of phase-pure, crystalline lithium silicides Li_xSi (x = 4.4, 3.75, 3.25, and 2.33). The important contributions and findings of this work are as follows.

Synthesis. The use of a low-boiling-point lubricant hexane during the high-energy ball-milling synthesis enables an easy purification of Li_xSi. Except $Li_{3.75}Si$, all other phases require 10% of extra Li in molar ratio beyond the stoichiometry. A postannealing treatment is also needed for making $Li_{3.25}Si$. In addition, Li grains cannot be replaced by LiH powders.

Crystal Structure of $Li_{3.75}Si$. All XRD peaks from $Li_{3.75}Si$ appear at smaller diffraction angles than those from the electrochemically synthesized $Li_{3.75}Si$. This indicates that atomic distances in our $Li_{3.75}Si$ are larger than those of the electrochemically synthesized $Li_{3.75}Si$. The reason is assigned to the smaller internal pressures (or stress) in the ball-milling synthesis than in the electrochemical synthesis.

Chemical Stability and Thermal Stability of $Li_{4.4}Si$ and $Li_{3.75}Si$. $Li_{4.4}Si$ and $Li_{3.75}Si$ are subject to chemical reactions on their surfaces in the presence of certain battery-assembly-related chemicals. $Li_{4.4}Si$ is stable up to 300−350 °C and $Li_{3.75}Si$ is stable up to 150−200 °C, depending on the annealing durations. Above the threshold temperature, both phases are converted to $Li_{3.25}Si$. This study indicates that $Li_{4.4}Si$ and $Li_{3.75}Si$ will be robust in the case of battery thermal runaway. The remarkable thermal stability of the widely believed metastable phase $Li_{3.75}Si$ may motivate more systematic studies on the different physicochemical properties of this compound synthesized by different methods.

C Encapsulation. The attempt to encapsulate $Li_{4.4}Si$ with a C matrix causes conversion of $Li_{4.4}Si$ to $Li_{2.33}Si$ after they were annealed in a PAN slurry. Although this degradation is undesirable, the resultant composites still hold the promise for being high performance electrodes, as the carbon matrix may compensate for the deficient void space provided by Li. The verification assessment is underway and will be published separately.

EXPERIMENTAL SECTION

Chemicals. Lithium metal (Li; granular 4−10 mesh 99%), silicon (Si; 325 mesh 99%), hexane (anhydrous, 95%), toluene (anhydrous, 99.8%), dodecane (anhydrous, ≥ 99%), *N*,*N*-dimethylformamide (DMF; anhydrous, 99.8%), polyacrylonitrile (PAN; $M_w \approx$ 150K), ethylenecarbonate (EC; anhydrous 99%, solid), and diethylcarbonate (DEC; anhydrous 99%) were purchased from Aldrich. The LP40 electrolyte [1 M lithium hexafluorophosphate ($LiPF_6$) in 1/1 EC/DEC] was purchased from BASF. All chemicals were used as received and were opened and stored in an argon-filled glovebox (H_2O < 0.5 ppm and O_2 < 1 ppm).

Synthesis. The synthesis of lithium silicides (Li_xSi) was adapted from a literature method.[28,61] All Li_xSi compounds, except $Li_{3.25}Si$, were produced directly from the ball mill, requiring no postannealing. Stoichiometric amounts of Li grains and Si powders were loaded in a stainless steel ball mill jar in an argon-filled glovebox (MBraun LABstar MB10 compact) and then mounted in a high-energy ball mill (SPEX, Mixer/Mill 8000M) outside of the glovebox. The milling duration was usually 100 min. Typically, hexane was added as a lubricant to prevent Li from sticking to the balls and jar. To obtain pure $L_{4.4}Si$, 10% of extra Li was required. A typical mass loading was as follows: 0.2200 g of Li, 0.1839 g of Si, and 3 mL of hexane. After milling, the jar was transferred back into the glovebox. The hexane was evaporated away, resulting in a black powder product. The synthesis of pure $Li_{3.25}Si$ required an additional annealing step; that is, the obtained powder after ball milling was heated at 600 °C for 1 h at a 10 °C/min ramping rate in a tube furnace under an argon flow. Typically, a magnet was used to attract Fe debris out of as-synthesized samples before further analysis/use.

Chemical Stability of $Li_{4.4}Si$ and $Li_{3.75}Si$. The as-synthesized $Li_{4.4}Si$ powder (or $Li_{3.75}Si$) was immersed in several chemicals overnight with mechanical stirring. These chemicals were DEC, a mixture of EC and DEC at a weight ratio of 1/1, and the LP40 electrolyte. EC could not be directly used for this study because of its solid nature at room temperature. The treated product was then collected via centrifugation and washed with the respective solvent in each system. After evaporation of the washing solvent, the obtained sample was ready for characterization.

Thermal Stability of $Li_{4.4}Si$ and $Li_{3.75}Si$. The as-synthesized $Li_{4.4}Si$ powder (or $Li_{3.75}Si$) was loaded into a closed stainless steel jar in argon. Then, the sample jar was heated at various temperatures (200−600 °C for $Li_{4.4}Si$ and 100−350 °C for $Li_{3.75}Si$) for various durations (1, 6, and 12 h) at a ramping rate of 10 °C/min in a tube furnace under an argon flow. Afterward, the annealed sample was collected in a glovebox for further analysis.

C Encapsulation of $Li_{4.4}Si$ and $Li_{3.25}Si$. Using the synthesized $Li_{4.4}Si$ powder, a slurry comprised of $Li_{4.4}Si$ and PAN at a 3.3/1 ratio (70/30 Si/C) in DMF was made. First 26.2 mg of PAN was dissolved into 1 mL of DMF. Then 86.5 mg of the synthesized $Li_{4.4}Si$ was added, and the solution was stirred for 3 h. The slurry was spread onto Cu foil and dried at 80 °C for 2 h. The film of $Li_{4.4}Si$/PAN on Cu foil was loaded into a stainless steel container and heated at 250 °C for 30 min, followed by 300 °C for 60 min in a tube furnace under argon (at a 10 °C/min ramping rate). The resulting $Li_{4.4}Si$/resilient C composite was stored in an argon glovebox for characterization.

Analysis and Characterization. XRD profiles were acquired on a Philips X'Pert X-ray diffractometer, for which the samples were prepared in an argon-filled glovebox by transferring the purified product onto a glass substrate and then covering it with a drop of mineral oil to prevent detrimental reactions with air during the measurement. The mineral oil contributed a smooth and broad peak centered at 17.2° spanning from 10 to 25°; this interference was eliminated through background subtraction. TEM images and EDX spectra were obtained on a Philips CM200 microscope with a built-in EDX detector (Princeton Gamma-Tech Prism). The TEM samples were prepared by dropping the sample solutions onto 400-mesh Cu grids (from Electron Microscopy Sciences) and dried in a glovebox. A FTIR spectrometer (Thermo Scientific Nicolet iS50) was used to measure the FTIR spectra using the attenuated total reflection (ATR) accessory at a spectral resolution of 2 cm^{-1}. Solid-state ^{7}Li NMR experiments were performed on a Bruker 400 MHz spectrometer with a ^{7}Li operating frequency of 155.3 MHz. Spectra were obtained by transforming the resulting free-induction decay of a single $\pi/2$ (5 μs) pulse sequence. All spectra were acquired by loading the sample in a 4 mm rotor and using the magic-angle-spinning technique at 12 kHz. LiCl solid powder was used as the reference to set the chemical shift of its Li^{+} as 0 ppm.

■ ASSOCIATED CONTENT

Supporting Information

Two videos, XRD data of various ball-mill-synthesized products, comparison of XRD data between our product and literature work, FTIR spectra of several standard chemicals, and XRD data and Raman spectra of annealed products from mixtures of $Li_{4.4}Si$ and PAN powders. This material is available free of charge via the Internet at http://pubs.acs.org.

■ AUTHOR INFORMATION

Corresponding Author

*E-mail: yonyang@mines.edu. Fax: 1-303-273-3629. Tel: 1-303-384-2389.

Author Contributions

‡The manuscript was written through contributions of all authors. All authors have given approval to the final version of the manuscript. These authors contributed equally.

Notes

The authors declare no competing financial interest.

■ ACKNOWLEDGMENTS

This work is supported by the Startup Fund for Y.Y. from Colorado School of Mines (CSM) and the proof-of-concept Grant 11833 jointly sponsored by the Colorado Office of Economic Development and International Trade and the Office of Technology Transfer of CSM.

■ REFERENCES

(1) Boukamp, B. A.; Lesh, G. C.; Huggins, R. A. *J. Electrochem. Soc.* **1981**, *128*, 725−729.
(2) Graetz, J.; Ahn, C. C.; Yazami, R.; Fultz, B. *Electrochem. Solid State* **2003**, *6*, A194−A197.
(3) Yazami, R.; Touzain, P. *J. Power Sources* **1983**, *9*, 365−371.
(4) Liu, X. H.; Liu, Y.; Kushima, A.; Zhang, S. L.; Zhu, T.; Li, J.; Huang, J. Y. *Adv. Energy Mater.* **2012**, *2*, 722−741.
(5) Wu, H.; Yu, G.; Pan, L.; Liu, N.; McDowell, M. T.; Bao, Z.; Cui, Y. *Nat. Commun.* **2013**, *4*, Article No. 1943.
(6) Liu, N.; Wu, H.; McDowell, M. T.; Yao, Y.; Wang, C. M.; Cui, Y. *Nano Lett.* **2012**, *12*, 3315−3321.
(7) Wu, H.; Chan, G.; Choi, J. W.; Ryu, I.; Yao, Y.; McDowell, M. T.; Lee, S. W.; Jackson, A.; Yang, Y.; Hu, L. B.; Cui, Y. *Nat. Nanotechnol.* **2012**, *7*, 309−314.
(8) Yoshio, M.; Wang, H. Y.; Fukuda, K.; Umeno, T.; Dimov, N.; Ogumi, Z. *J. Electrochem. Soc.* **2002**, *149*, A1598−A1603.
(9) Xiao, J.; Xu, W.; Wang, D.; Choi, D.; Wang, W.; Li, X.; Graff, G. L.; Liu, J.; Zhang, J.-G. *J. Electrochem. Soc.* **2010**, *157*, A1047−A1051.
(10) Chan, C. K.; Peng, H. L.; Liu, G.; McIlwrath, K.; Zhang, X. F.; Huggins, R. A.; Cui, Y. *Nat. Nanotechnol.* **2008**, *3*, 31−35.
(11) Baggetto, L.; Notten, P. H. L. *J. Electrochem. Soc.* **2009**, *156*, A169−A175.
(12) Wang, B.; Luo, B.; Li, X.; Zhi, L. *Mater. Today* **2012**, *15*, 544−552.
(13) Courtney, I. A.; Dahn, J. R. *J. Electrochem. Soc.* **1997**, *144*, 2045−2052.
(14) Arreaga-Salas, D. E.; Sra, A. K.; Roodenko, K.; Chabal, Y. J.; Hinkle, C. L. *J. Phys. Chem. C* **2012**, *116*, 9072−9077.
(15) Chan, C. K.; Ruffo, R.; Hong, S. S.; Cui, Y. *J. Power Sources* **2009**, *189*, 1132−1140.
(16) Kasavajjula, U.; Wang, C. S.; Appleby, A. J. *J. Power Sources* **2007**, *163*, 1003−1039.
(17) Ryu, J. H.; Kim, J. W.; Sung, Y. E.; Oh, S. M. *Electrochem. Solid State* **2004**, *7*, A306−A309.
(18) Liu, X. H.; Wang, J. W.; Huang, S.; Fan, F. F.; Huang, X.; Liu, Y.; Krylyuk, S.; Yoo, J.; Dayeh, S. A.; Davydov, A. V.; Mao, S. X.; Picraux, S. T.; Zhang, S. L.; Li, J.; Zhu, T.; Huang, J. Y. *Nat. Nanotechnol.* **2012**, *7*, 749−756.
(19) Liu, X. H.; Huang, J. Y. *Energy Environ. Sci.* **2011**, *4*, 3844−3860.
(20) Liu, X. H.; Zhong, L.; Huang, S.; Mao, S. X.; Zhu, T.; Huang, J. Y. *ACS Nano* **2012**, *6*, 1522−1531.
(21) McDowell, M. T.; Ryu, I.; Lee, S. W.; Wang, C. M.; Nix, W. D.; Cui, Y. *Adv. Mater.* **2012**, *24*, 6034−6041.
(22) McDowell, M. T.; Lee, S. W.; Harris, J. T.; Korgel, B. A.; Wang, C. M.; Nix, W. D.; Cui, Y. *Nano Lett.* **2013**, *13*, 758−764.
(23) Wang, J. W.; He, Y.; Fan, F. F.; Liu, X. H.; Xia, S. M.; Liu, Y.; Harris, C. T.; Li, H.; Huang, J. Y.; Mao, S. X.; Zhu, T. *Nano Lett.* **2013**, *13*, 709−715.
(24) Wang, C. M.; Li, X. L.; Wang, Z. G.; Xu, W.; Liu, J.; Gao, F.; Kovarik, L.; Zhang, J. G.; Howe, J.; Burton, D. J.; Liu, Z. Y.; Xiao, X. C.; Thevuthasan, S.; Baer, D. R. *Nano Lett.* **2012**, *12*, 1624−1632.
(25) Liu, X. H.; Zhang, L. Q.; Zhong, L.; Liu, Y.; Zheng, H.; Wang, J. W.; Cho, J. H.; Dayeh, S. A.; Picraux, S. T.; Sullivan, J. P.; Mao, S. X.; Ye, Z. Z.; Huang, J. Y. *Nano Lett.* **2011**, *11*, 2251−2258.
(26) Okamoto, H. *J. Phase Equilib. Diff.* **2009**, *30*, 118−119.
(27) Misra, S.; Liu, N.; Nelson, J.; Hong, S. S.; Cui, Y.; Toney, M. F. *ACS Nano* **2012**, *6*, 5465−5473.
(28) Key, B.; Bhattacharyya, R.; Morcrette, M.; Seznec, V.; Tarascon, J. M.; Grey, C. P. *J. Am. Chem. Soc.* **2009**, *131*, 9239−9249.
(29) Hatchard, T. D.; Dahn, J. R. *J. Electrochem. Soc.* **2004**, *151*, A838−A842.
(30) Li, J.; Dahn, J. R. *J. Electrochem. Soc.* **2007**, *154*, A156−A161.
(31) Kang, K.; Lee, H. S.; Han, D. W.; Kim, G. S.; Lee, D.; Lee, G.; Kang, Y. M.; Jo, M. H. *Appl. Phys. Lett.* **2010**, *96*, 053110.
(32) Ghassemi, H.; Au, M.; Chen, N.; Heiden, P. A.; Yassar, R. S. *ACS Nano* **2011**, *5*, 7805−7811.
(33) Wang, C.; Wu, H.; Chen, Z.; McDowell, M. T.; Cui, Y.; Bao, Z. *Nat. Chem.* **2013**, *5*, 1042−1048.
(34) Wang, F.; Wu, L. J.; Key, B.; Yang, X. Q.; Grey, C. P.; Zhu, Y. M.; Graetz, J. *Adv. Energy Mater.* **2013**, *3*, 1324−1331.
(35) Piper, D. M.; Yersak, T. A.; Son, S. B.; Kim, S. C.; Kang, C. S.; Oh, K. H.; Ban, C. M.; Dillon, A. C.; Lee, S. H. *Adv. Energy Mater.* **2013**, *3*, 697−702.
(36) Hertzberg, B.; Alexeev, A.; Yushin, G. *J. Am. Chem. Soc.* **2010**, *132*, 8548−8549.
(37) Ogata, K.; Salager, E.; Kerr, C. J.; Fraser, A. E.; Ducati, C.; Morris, A. J.; Hofmann, S.; Grey, C. P. *Nat. Commun.* **2014**, *5*, Article No. 3217.
(38) Liu, N.; Hu, L.; McDowell, M. T.; Jackson, A.; Cui, Y. *ACS Nano* **2011**, *5*, 6487−6493.
(39) Datta, M. K.; Kumta, P. N. *J. Power Sources* **2009**, *194*, 1043−1052.

(40) Hassoun, J.; Kim, J.; Lee, D. J.; Jung, H. G.; Lee, S. M.; Sun, Y. K.; Scrosati, B. *J. Power Sources* **2012**, *202*, 308−313.
(41) Yan, Y.; Yin, Y. X.; Xin, S.; Su, J.; Guo, Y. G.; Wan, L. J. *Electrochim. Acta* **2013**, *91*, 58−61.
(42) Elazari, R.; Salitra, G.; Gershinsky, G.; Garsuch, A.; Panchenko, A.; Aurbach, D. *Electrochem. Commun.* **2012**, *14*, 21−24.
(43) Zeng, Z. D.; Liu, N.; Zeng, Q. S.; Ding, Y.; Qu, S. X.; Cui, Y.; Mao, W. L. *J. Power Sources* **2013**, *242*, 732−735.
(44) Lee, J. K.; Kung, M. C.; Trahey, L.; Missaghi, M. N.; Kung, H. H. *Chem. Mater.* **2009**, *21*, 6−8.
(45) Hwa, Y.; Kim, W. S.; Hong, S. H.; Sohn, H. J. *Electrochim. Acta* **2012**, *71*, 201−205.
(46) Cui, L. F.; Ruffo, R.; Chan, C. K.; Peng, H. L.; Cui, Y. *Nano Lett.* **2009**, *9*, 491−495.
(47) Guo, J. C.; Chen, X. L.; Wang, C. S. *J. Mater. Chem.* **2010**, *20*, 5035−5040.
(48) Ng, S. H.; Wang, J. Z.; Wexler, D.; Konstantinov, K.; Guo, Z. P.; Liu, H. K. *Angew. Chem., Int. Ed.* **2006**, *45*, 6896−6899.
(49) Li, X. L.; Meduri, P.; Chen, X. L.; Qi, W.; Engelhard, M. H.; Xu, W.; Ding, F.; Xiao, J.; Wang, W.; Wang, C. M.; Zhang, J. G.; Liu, J. *J. Mater. Chem.* **2012**, *22*, 11014−11017.
(50) Luo, J. Y.; Zhao, X.; Wu, J. S.; Jang, H. D.; Kung, H. H.; Huang, J. X. *J. Phys. Chem. Lett.* **2012**, *3*, 1824−1829.
(51) He, Y. S.; Gao, P. F.; Chen, J.; Yang, X. W.; Liao, X. Z.; Yang, J.; Ma, Z. F. *RSC Adv.* **2011**, *1*, 958−960.
(52) Usui, H.; Nomura, M.; Nishino, H.; Kusatsu, M.; Murota, T.; Sakaguchi, H. *Mater. Lett.* **2014**, *130*, 61−64.
(53) Guo, J.; Xu, Y.; Wang, C. *Nano Lett.* **2011**, *11*, 4288−4294.
(54) Guo, J.; Yang, Z.; Yu, Y.; Abruña, H. D.; Archer, L. A. *J. Am. Chem. Soc.* **2013**, *135*, 763−767.
(55) Chung, Y. S.; Yoo, S. H.; Kim, C. K. *Ind. Eng. Chem. Res.* **2009**, *48*, 4346−4351.
(56) Sohn, J. Y.; Gwon, S. J.; Choi, J. H.; Shin, J.; Nho, Y. C. *Nucl. Instrum. Methods Phys. Res., Sect. B* **2008**, *266*, 4994−5000.
(57) Liu, B.; Soares, P.; Checkles, C.; Zhao, Y.; Yu, G. *Nano Lett.* **2013**, *13*, 3414−3419.
(58) Peled, E. *J. Electrochem. Soc.* **1979**, *126*, 2047−2051.
(59) Nesper, R.; von Schnering, H. G. *J. Solid State Chem.* **1987**, *70*, 48−57.
(60) Dupke, S.; Langer, T.; Pottgen, R.; Winter, M.; Eckert, H. *Solid State Nucl. Magn. Reson.* **2012**, *42*, 17−25.
(61) Dupke, S.; Langer, T.; Pottgen, R.; Winter, M.; Passerini, S.; Eckert, H. *Phys. Chem. Chem. Phys.* **2012**, *14*, 6496−6508.
(62) Ma, R. J.; Liu, Y. F.; He, Y. P.; Gao, M. X.; Pan, H. G. *J. Phys. Chem. Lett.* **2012**, *3*, 3555−3558.
(63) Tamori, R.; Machida, N.; Shigematsu, T. *J. Jpn. Soc. Powder Powder Metall.* **2001**, *48*, 267−273.
(64) Jain, A.; Kawasako, E.; Miyaoka, H.; Ma, T.; Isobe, S.; Ichikawa, T.; Kojima, Y. *J. Phys. Chem. C* **2013**, *117*, 5650−5657.
(65) Zeilinger, M.; Kurylyshyn, I. M.; Haussermann, U.; Fassler, T. F. *Chem. Mater.* **2013**, *25*, 4623−4632.
(66) Zeilinger, M.; Benson, D.; Haussermann, U.; Fassler, T. F. *Chem. Mater.* **2013**, *25*, 1960−1967.
(67) Yang, Y. A.; Taggart, D. K.; Brown, M. A.; Xiang, C. X.; Kung, S. C.; Yang, F.; Hemminger, J. C.; Penner, R. M. *ACS Nano* **2009**, *3*, 4144−4154.
(68) Wang, Y. D.; Dahn, J. *J. Electrochem. Soc.* **2006**, *153*, A2314−A2318.
(69) Hashimoto, Y.; Machida, N.; Shigematsu, T. *Solid State Ionics* **2004**, *175*, 177−180.
(70) Nie, M.; Abraham, D. P.; Chen, Y.; Bose, A.; Lucht, B. L. *J. Phys. Chem. C* **2013**, *117*, 13403−13412.
(71) Philippe, B.; Dedryvere, R.; Gorgoi, M.; Rensmo, H.; Gonbeau, D.; Edstrom, K. *Chem. Mater.* **2013**, *25*, 394−404.
(72) Trill, J. H.; Tao, C. Q.; Winter, M.; Passerini, S.; Eckert, H. *J. Solid State Electrochem.* **2011**, *15*, 349−356.
(73) Zhu, M.; Weber, C. J.; Yang, Y.; Konuma, M.; Starke, U.; Kern, K.; Bittner, A. M. *Carbon* **2008**, *46*, 1829−1840.
(74) Jiang, Q.; Zhang, S.; Zhao, M. *Mater. Chem. Phys.* **2003**, *82*, 225−227.
(75) Obrovac, M. N.; Christensen, L. *Electrochem. Solid State* **2004**, *7*, A93−A96.
(76) Jung, H. J.; Park, M.; Han, S. H.; Lim, H.; Joo, S. K. *Solid State Commun.* **2003**, *125*, 387−390.
(77) Baggetto, L.; Niessen, R. A. H.; Roozeboom, F.; Notten, P. H. L. *Adv. Funct. Mater.* **2008**, *18*, 1057−1066.
(78) Chakrapani, V.; Rusli, F.; Filler, M. A.; Kohl, P. A. *J. Power Sources* **2012**, *205*, 433−438.